# Dynamics of deep soil carbon – insights from ^{14}C time-series across a climatic gradient

Tessa Sophia van der Voort[1,†], Utsav Mannu[1, †], Frank Hagedorn[2], Cameron McIntyre[1,3], Lorenz Walthert[2], Patrick Schleppi[2], Negar Haghipour[1], Timothy Ian Eglinton[1]

[1]Institute of Geology, ETH Zürich, Sonneggstrasse 5, 8092 Zürich, Switzerland
[2]Forest soils and Biogeochemistry, Swiss Federal Research Institute WSL, Zürcherstrasse 111, 8903 Birmensdorf, Switzerland
[3]Department of Physics, Laboratory of Ion Beam Physics, ETH Zurich, Schaffmattstrasse 20, 9083 Zurich
[†] New address: Campus Fryslân, University of Groningen, Wirdumerdijk 34, Leeuwarden
[††]New address: Department of Earth and Climate Science, IISER Pune, Pune, India

*correspondence to*: Tessa Sophia van der Voort (tessa.vandervoort@erdw.ethz.ch)

**Abstract.** Quantitative constraints on soil organic matter (SOM) dynamics are essential for comprehensive understanding of the terrestrial carbon cycle. Deep soil carbon is of particular interest, as it represents large stocks and its turnover times remain highly uncertain. In this study, SOM dynamics in both the top and deep soil across a climatic (average temperature ~1-9 °C) gradient are determined using time-series (~20 years) ^{14}C data from bulk soil and water-extractable organic carbon (WEOC). Analytical measurements reveal enrichment of bomb-derived radiocarbon in the deep soil layers on the bulk level during the last two decades. The WEOC pool is strongly enriched in bomb-derived carbon, indicating that it is a dynamic pool. Turnover time estimates of both the bulk and WEOC pool show that the latter cycles up to a magnitude faster than the former. The presence of bomb-derived carbon in the deep soil, as well as the rapidly turning WEOC pool across the climatic gradient implies that there likely is a dynamic component of carbon in the deep soil. Precipitation and bedrock type appear to exert a stronger influence on soil C turnover time and stocks as compared to temperature.

## 1 Introduction

Within the broad societal challenges accompanying climate and land use change, a better understanding of the drivers of carbon turnover time in the largest terrestrial reservoir of organic carbon, as constituted by soil organic matter (SOM), is essential (Batjes, 1996; Davidson and Janssens, 2006; Doetterl et al., 2015; Prietzel et al., 2016). Terrestrial carbon turnover time remains one of the largest uncertainties in climate model predictions (Carvalhais et al., 2014; He et al., 2016). At present, there is no consensus on the net effect that climate and land use change will have on SOM stocks (Crowther et al., 2016; Gosheva et al., 2017; Melillo et al., 2002; Schimel et al., 2001; Trumbore and Czimczik, 2008). Deep soil carbon is of particular interest because of its large stocks (Jobbagy and Jackson, 2000; Balesdent et al., 2018; Rumpel and Kogel-Knabner, 2011) and perceived stability. The stability is indicated by low ^{14}C content (Rethemeyer et al., 2005; Schrumpf et al., 2013; van der Voort et al., 2016) and low microbial activity (Fierer et al., 2003). Despite its importance, deep soil carbon has not been frequently studied and remains poorly understood (Angst et al., 2016; Mathieu et al., 2016; Rumpel and Kogel-Knabner, 2011). The inherent complexity of SOM and the multitude of drivers controlling its stability further impedes the understanding of this globally significant carbon pool (Schmidt et al., 2011). In this framework, there is a particular interest in the portion of soil carbon that could be most vulnerable to change, especially in colder climates (Crowther et al., 2016). Water-exactable organic carbon (WEOC) is seen as a dynamic and potentially vulnerable carbon pool in the soil (Hagedorn et al., 2004; Lechleitner et al., 2016). Radiocarbon (^{14}C) can be a

44  powerful tool to determine the dynamics of carbon turnover time over decadal to millennial timescales because
45  of the incorporation of bomb-derived $^{14}C$ introduced in the atmosphere in the 1950's as well as the radioactive
46  decay of $^{14}C$ naturally present in the atmosphere (Torn et al., 2009). Furthermore, $^{14}C$ can also be employed to
47  identify petrogenic (or geogenic) carbon in the soil profile. Understanding the potential mobilization of stabilized
48  petrogenic carbon is key because it could constitute an additional $CO_2$ source to the atmosphere (Hemingway et
49  al., 2018). Time-series $^{14}C$ data is particularly insightful because it enables the tracking of recent decadal carbon.
50  Furthermore, single time-point $^{14}C$ data can yield two estimates for turnover time, whilst time-series data yields a
51  single turnover time estimate (Torn et al., 2009). Given that the so-called "bomb radiocarbon spike" will continue
52  to diminish in the coming decades, time-series measurements are increasingly a matter of urgency in order to take
53  full advantage of this intrinsic tracer (Graven, 2015). Several case-studies have collected time-series $^{14}C$ soil
54  datasets and demonstrated the value of this approach (Baisden and Parfitt, 2007; Prior et al., 2007; Fröberg et al.,
55  2010; Mills et al., 2013, Schrumpf and Kaiser, 2015). However, these studies are rare, based on specific single
56  sites and have been rarely linked to abiotic and biotic parameters. Much more is yet to be learned about the carbon
57  cycling through time-series observations in top- and subsoils along environmental gradients. Furthermore, to our
58  knowledge, there are no studies with pool-specific $^{14}C$ soil time-series focusing on labile carbon.
59
60  This study assesses two-pool soil carbon dynamics as determined by time-series (~20 years) radiocarbon across a
61  climatic gradient. The time-series data is analyzed by a numerically optimized model with a robust error reduction
62  to yield carbon turnover time estimates for the bulk and dynamic WEOC pool. Model output is linked to potential
63  drivers such as climate, forest productivity and physico-chemical soil properties. The overall objective of this
64  study is to improve our understanding of shallow and deep soil carbon dynamics in a wide range of ecosystems.
65

## 2 Materials and methods

### 2.1 Study sites, sampling strategy and WEOC extraction

68  The five sites investigated in this study are located in Switzerland between 46-47° N and 6-10° E and encompass
69  large climatic (mean annual temperature (MAT) 1.3-9.2°C, mean annual precipitation (MAP) 864-2126 mm m$^{-}$
70  $^2$y$^{-1}$) and geological gradients (Table 1). The sites are part of the Long-term Forest Ecosystem Research program
71  (LWF) at the Swiss Federal Institute for Forest, Snow and Landscape Research, WSL (Schaub et al., 2011; Etzold
72  et al., 2014). The soils of these sites were sampled between 1995 and 1998 (Walthert et al., 2002, 2003) and were
73  re-sampled following the same sampling strategy in 2014 with the aim to minimize noise caused by small-scale
74  soil heterogeneity. In both instances sixteen samples were taken on a regular grid on the identical 43 by 43 meters
75  (~1600 m$^2$) plot (Fig. 1; see Van der Voort et al., 2016 for further details). For the archived samples taken between
76  1995 and 1998, mineral soil samples down to 40 cm depth (intervals of 0-5, 5-10, 10-20 and 20-40 cm) were taken
77  on an area of 0.5 by 0.5 m (0.25 m$^2$). For samples >40 cm (intervals of 40-60, 60-80 and 80-100 cm), corers were
78  used to acquire samples (n=5 in every pit, area ~2.8×10$^{-3}$ m$^2$). The organic layer was sampled by use of a metal
79  frame (30×30 cm). The samples were dried at 35-40°C, sieved to remove coarse material (2 mm), and stored in
80  hard plastic containers under controlled climate conditions in the "Pedothek" at WSL (Walthert et al., 2002). For
81  the samples acquired in 2014 the same sampling strategy was followed, and samples were taken on the exact same
82  plot proximal (~10 m) to the legacy samples. For the sampling, a SHK Martin Burch AG HUMAX soil corer
83  (~2×10$^{-3}$ m$^2$) was used for all depths (0-100 cm). For the organic layer, a metal frame of 20×20 cm was used to

84    sample. Samples were sieved (2 mm), frozen and freeze-dried using an oil-free vacuum-pump powered freeze

85    dryer (Christ, Alpha 1-4 LO *plus*). For the time-series radiocarbon measurements, all samples covering ~1600 m$^2$

86    were pooled to one composite sample per soil depth using the bulk-density. In order to determine bulk-density of

87    the fine earth of the 2014 samples, stones > 2 mm were assumed to have a density of 2.65 g/cm$^3$. For the Alptal

88    site, sixteen cores were taken on a slightly smaller area (~1500 m$^2$) which encompasses the control plot of a

89    nitrogen addition experiment (NITREX project) (Schleppi et al., 1998). For this site, no archived samples are

90    available and thus only the 2014 samples were analyzed. Soil carbon stocks were estimated by multiplying SOC

91    concentrations with the mass of soil calculated from measured bulk densities and stone contents for each depth

92    interval (Gosheva et al., 2017). For the Nationalpark site, the soil carbon stocks from 80-100 cm were estimated

93    using data from a separately dug soil profile (Walthert et al., 2003) because the HUMAX corer could not penetrate

94    the rock-dense soil below 80 cm depth. In order to understand very deep soil carbon dynamics (i.e. >100 cm), this

95    study also includes single-time point $^{14}$C analyses of soil profiles that were dug down to the bedrock between

96    1995 and 1998 as part of the LWF programme on the same sites (Walthert et al., 2002). The sampling of the

97    profiles has not yet been repeated.

98

99    **2.2 Climate and soil data**

100   Temperature and precipitation data are derived from weather stations close to the study sites that have been

101   measuring for over two decades, yielding representative estimates of both variables and over the time period

102   concerned in this study (Etzold et al., 2014). The pH values for all sites and concerned depth intervals were

103   acquired during the initial sampling campaign (Walthert et al. 2002). At Alptal, pH values were determined as

104   described in Xu et al. (2009), values of 10-15 cm were extrapolated to the deeper horizons because of the uniform

105   nature of the Gley horizon. The Beatenberg Podzol is marked by strong elluviation (~4-35 cm) and illuviation

106   (~35-60 cm) (Walthert et al., 2003). Exchangeable cations were extracted (in triplicate) from the 2-mm-sieved

107   soil in an unbuffered solution of 1 M NH$_4$Cl for 1 hour on an end-over-end shaker using a soil-to-extract ratio of

108   1:10. The element concentrations in the extracts were determined by inductively coupled plasma atomic emission

109   spectroscopy (ICP-AES) (Optima 3000, Perkin–Elmer). Contents of exchangeable protons were calculated as the

110   difference between the total and the Al-induced exchangeable acidity as determined (in duplicate) by the KCl

111   method (Thomas, 1982). This method was applied only to soil samples with a pH (CaCl$_2$) < 6.5. In samples with

112   a higher pH, we assumed the quantities of exchangeable protons were negligible. The effective cation-exchange

113   capacity (CEC) was calculated by summing up the charge equivalents of exchangeable Na, K, Mg, Ca, Mn, Al,

114   Fe and H. The base saturation (BS) was defined as the percental fraction of exchangeable Na, K, Mg, and Ca of

115   the CEC (Walthert et al., 2002, 2013). Net primary production (NPP) was determined by Etzold et al. (2014) as

116   the sum of carbon fluxes by woody tree growth, foliage, fruit production and fine root production. Soil texture

117   (sand, silt and clay content) on plot-averaged samples taken in 2014 have been determined using grain size classes

118   for sand, silt and clay respectively of 0.05-2 mm, 0.002-0.05 mm and <0.002 mm according to Klute (1986). The

119   continuous distribution of grain sizes was also determined after removal of organic matter (350 °C for 12 h) using

120   the Mastersizer 2000 (Malvern Instruments Ltd.). Soil water potential (SWP) was measured on the same sites as

121   described in Von Arx et al., (2013). In accordance with Mathieu et al., (2015), topsoil refers to the mineral soil

122   up to 20 cm depth, and deep soil refers to mineral soil below 20 cm. Out of the five sites, two are hydromorphic

123     (Gleysol and Podzol in Alptal and Beatenberg respectively), whilst the others are non-hydromorphic (Luvisol,

124     Cambisol and Fluvisol in Othmarsingen, Lausanne and Nationalpark respectively).

125

126     **2.3 Isotopic ($^{14}$C, $^{13}$C) and compositional (C, N) analysis**

127     Prior to the isotopic analyses, inorganic carbon in all samples was removed by vapour acidification for 72 hours

128     (12M HCl) in desiccators at 60 °C (Komada et al., 2008). After fumigation, the acid was neutralised by substituting

129     NaOH pellets for another 48 hours. All glassware used during sample preparation was cleaned and combusted at

130     450°C for six hours prior to use. Water extractable organic carbon (WEOC) was procured by extracting dried soil

131     with of 0.5 wt% pre-combusted NaCl in ultrapure Milli-Q (MQ) water in a 1:4 soil:water mass ratio (adapted from

132     Hagedorn et al., (2004), details in Lechleitner et al., (2016)).

133     In order to determine absolute organic carbon and nitrogen content as well as $^{13}$C values, an Elemental Analyser-

134     Isotope Ratio Mass Spectrometer system was used (EA-IRMS, Elementar, vario MICRO cube – Isoprime, Vison).

135     Atropine (Säntis) and an in-house standard peptone (Sigma) were used for the calibration of the EA-IRMS for

136     respectively carbon concentration, nitrogen concentration and C:N ratios and $^{13}$C. High $^{13}$C values were used to

137     flag if all inorganic carbon had been removed by acidification.

138     For the $^{14}$C measurements of the bulk soil samples were first graphitised using an EA-AGE (elemental analyser-

139     automated graphitization equipment, Ionplus AG) system at the Laboratory of Ion Beam Physics at ETH Zürich

140     (Wacker et al., 2009). Graphite samples were measured on a MICADAS (MIniturised radioCArbon DAting

141     System, Ionplus AG) also at the Laboratory of Ion Beam Physics, ETH Zürich (Wacker et al., 2010). For three

142     samples (Alptal depth intervals 40-60, 60-80 and 80-100 cm) the $^{14}$C signature was directly measured as $CO_2$ gas

143     using the recently developed online elemental analyzer (EA) - stable isotope ratio mass spectrometers (IRMS)–

144     AMS system et ETH Zürich (McIntyre et al., 2016). Oxalic acid (NIST SRM 4990C) was used as the normalising

145     standard. Phthalic anhydride and in-house anthracite coal were used as blank. Two in-house soil standards (Alptal

146     soil 0-5 cm, Othmarsingen soil 0-5 cm) were used as secondary standards. For the WEOC, samples were converted

147     to $CO_2$ by Wet Chemical Oxidation (WCO) (Lang et al., 2016) and run on the AMS using a Gas Ion Source (GIS)

148     interface (Ionplus). To correct for contamination, a range of modern standards (sucrose, Sigma, δ13C = -12.4 ‰

149     VPDB, F$^{14}$C = 1.053 ± 0.003) and fossil standards (phthalic acid, Sigma, δ13C = -33.6‰ VPDB, F$^{14}$C <0.0025)

150     were used (Lechleitner et al., 2016).

151

152

### 2.4 Numerical optimization to find carbon turnover time and size of the dynamic pool

#### 2.4.1 Turnover time based on a single ¹⁴C measurement

The ¹⁴C signature of a sample can be used to estimate turnover time of a carbon pool (Torn et al., 2009).

$$R_{sample,t} = k \times R_{atm,t} + (1 - k - \lambda) \times R_{sample(t-1)} \quad (1)$$

$$R_{sample,t} = \frac{\Delta^{14}C_{sample}}{1000} + 1 \quad (2)$$

In Eq. 1-2, the constant for radioactive decay of ¹⁴C is indicated as $\lambda$, the decomposition rate $k$ (inverse of turnover time) is the only unknown in this equation and is hence the variable for which the optimal value that fits the data is sought using the model. The $R$ value of the sample is inferred from $\Delta^{14}$C, hence accounting for the sampling year, as shown in Eq. (2) (Herold et al., 2014; Solly et al., 2013). In order to avoid ambiguity, the term *turnover time* and not i.e. mean residence time is used solely in this manuscript (Sierra et al., 2016).

For the turnover time estimation, we assumed the system to be in steady state over the modeled period (~1×10⁴ years, indicating soil formation since the last glacial retreat (Ivy-Ochs et al., 2009)), hence accounting both for radioactive decay and incorporation of the bomb-testing derived material produced in the 1950's and 1960's (Eq. 1.) (Herold et al., 2014; Torn et al., 2009). We assumed an initial fraction modern (Fm) of ¹⁴C value of 1 at 10000 B.C.. For the period after 1900 atmospheric fraction modern (Fm) values of the Northern Hemisphere were used (Hua et al., 2013). This equation could be solved in Excel with manual iterations (e.g. Herold et al., 2014), or alternatively a numerical optimization can be used to find the best fit automatically. In this paper, we used a numerical optimization constructed in MATLAB version 2015a (The MathWorks, Inc., Natick, Massachusetts, United States) to find the best fit. The numerical optimization is exhaustive, meaning that every single turnover time value from 1 to 10.000 years with an interval of 0.1 year is tested. The error is defined as the difference between the fitted value of R and the measured value (Eq. 3). The turnover time value with the lowest error is then automatically selected.

$$Error_{single\ timepoint} = |R_{calculated} - R_{measured}| \quad (3)$$

The residual error of each fit are provided in the Supplemental Information (SI) Table 3. Turnover times determined with the numerical optimization match the manually optimized turnover time modeling published previously (Herold et al., 2014; Solly et al., 2013).

#### 2.4.2 Turnover time based on two ¹⁴C measurements

A single ¹⁴C value could yield possible turnover time values (Torn et al., 2009, Graven et al., 2015). If there is a time-series ¹⁴C dataset, this problem can be eliminated. In this paper, we have time-series data of both the bulk soil, as well as the vulnerable fraction (WEOC). For all samples a time-series dataset is available, both data points are employed to give the best estimate of turnover time. The same numerical optimization (Eq. 1 and 2) as we did for a single time-point, except that we try to find the best fit for both time points whilst reducing the compounding residual mean square error (RSME, Eq. 4). As can be seen in Fig. 2a, single time points can yield two likely

turnover times but when two datapoints are available, a single value can be found. The input data for Figure 2 can be found in SI Table 1. The results of the time-series turnover time modelling for both the bulk and WEOC pool of the sub-alpine site Beatenberg are shown in Fig. 3.

$$Error_{two\ timepoints} = \sqrt[2]{|R_{calculated} - R_{measured}|^2_{time\ point\ 1} + |R_{calculated} - R_{measured}|^2_{time\ point\ 1}} \quad (4)$$

### 2.4.3 Vegetation-induced lag

In order to account for vegetation-lag, two scenarios were run: firstly (1) with no assumed lag between the fixation of carbon from the atmosphere and input into to the soil and (2) model run with a lag of fixation of the atmospheric carbon as inferred from the dominant vegetation (Von Arx et al., 2013; Etzold et al., 2014). In the case of full deciduous trees coverage a lag of two years was assumed, and for the case of 100% conifer-dominated coverage a lag of 8 years was incorporated (Table 1).

### 2.4.4 Turnover time and size vulnerable pool based on two-pool model

As SOM is complex and composed of a continuum of pools with various ages (Schrumpf and Kaiser, 2015) and there is data available from two SOM pools, the $^{14}C$ time-series data can be leveraged to create a two-pool model. The following assumptions were made: First, both pools (slow & fast) make up the total carbon pool (Eq. 5). Secondly, the total turnover time of the bulk soil is made up out of the "dynamic" fraction turnover time multiplied by "dynamic" fraction pool size and the "slow" pool turnover time multiplied by "slow" pool size (Eq. 6). Furthermore, we assume that the signature of the sample (the time-series bulk data) is determined by the rate of incorporation of the material (atmospheric signal) and the loss of carbon the two pools (Eq. 7). Lastly, we assume that the radiocarbon signal of the WEOC pool is representative for a dynamic pool, as it could be representative for a larger component of rapidly turning over carbon, even in the deep soil (Baisden and Parfitt, 2007; Koarashi et al., 2012). The turnover time of the slow pool was set between 100 and 10.000 years, with a time-step of 10 years. The size of the dynamic pool was set to be between 0 and 0.5, with a size-step of 0.01.

$$1 = F_1 + F_2 \quad (5)$$

$$k_{total} = (F_1/k_1 + F_2/k_2)^{-1} \quad (6)$$

$$R_{sample,t} = k_{total} \times R_{atm,t} + F_1[(1 - k_1 - \lambda) \times R_{sample(t-1)}] + F_2(1 - k_2 - \lambda) \times R_{sample(t-1)} \quad (7)$$

Where $F_1$ is the relative size of the dynamic pool, and $F_2$ is the relative size of the (more) stable pool. The $k_1$ is the inverse of the turnover time of the dynamic or WEOC as determined using the numerical optimisation of Eq. 1-4. The $k_2$ is the inverse of the turnover time of the slow pool. The calculation of the error term becomes for complex because it needs to be recalculated for each unique combination of pool-size distribution (Eq. 5) and turnover time (inverse of $k$, Eq. 6). Therefore, the error space changes from column vector to a two-dimensional

218  matrix of length of the step size increments ($F_1$) and width of the inverse of the turnover time of the slow pool
219  ($k_2$).

220  $$Error_{k_2, F_1} = \sqrt[2]{|R_{calculated} - R_{measured}|^2_{time\ point\ 1} + |R_{calculated} - R_{measured}|^2_{time\ point\ 2}} \quad (8)$$

221  $$Error = Min(Error_{k_2, F_1}) \quad (9)$$

222  The numerical optimization finds the likeliest solution for the given dataset. This model constitutes a best fit, and
223  more data would better constrain the results. Additional details can be found in the Supplementary Information
224  (SI) text and SI Fig. 1. **All Matlab-based numerical optimization codes can be found in the SI**. For correlations
225  (packages HMISC, corrgram, method = pearson), statistical software R version 1.0.153 was used.
226

227  **3 Results**

228  **3.1 Changes of radiocarbon signatures over time**
229  Overall, there is a pronounced decrease in radiocarbon signature with soil depth at all sites (Fig. 4). The time-
230  series results show clear changes in radiocarbon signature over time from the initial sampling period (1995-1998)
231  as compared to 2014, with the magnitude of change depending on site and soil depth. In the uppermost 5 cm of
232  soils, the overarching trend in the bulk soil is a decrease in the $^{14}C$ bomb-spike signature in the warmer climates
233  (Othmarsingen, Lausanne), whilst at higher elevation (colder) sites (Beatenberg, Nationalpark) the bomb-derived
234  carbon appears to enter the top soil between 1995-8 and 2014.
235      Water-extractable OC (WEOC) has an atmospheric $^{14}C$ signature in the top soil at all sites in 2014. The
236  deep soil in the 1990's still has a negative $\Delta^{14}C$ signature of WEOC at multiple sites. There are two distinguishable
237  types of depth trends for WEOC in the 2014 dataset: (1) WEOC has the same approximate $^{14}C$ signature
238  throughout depth (Othmarsingen, Beatenberg), (2) WEOC becomes increasingly $^{14}C$ depleted with depth (Alptal,
239  Nationalpark), or an intermediate form where WEO$^{14}C$ is modern throughout the top soil but becomes more
240  depleted of $^{14}C$ in the deep soil (Lausanne) (Fig. 4). The isotopic trends of WEOC co-vary with grain size as
241  inherited from the bedrock type (Walthert et al., 2003). Soils with a relatively modern WEO$^{14}C$ signature in 2014
242  (down to 40 cm) are underlain by bedrock with large grained (SI Fig. 2, Table SI 3) components (the moraines
243  and sandstone at Othmarsingen, Lausanne and Beatenberg respectively). Soils where WEO$^{14}C$ signature decreases
244  with depth are underlain by bedrock containing fine-grained components. For instance, the Flysch in Alptal
245  (Schleppi et al., 1998) and intercalating layers of silt and coarse grained alluvial fan in Nationalpark (Walthert et
246  al., 2003) respectively.
247

248  **3.2 Carbon turnover time patterns**
249      Incorporation of a vegetation-induced time lag (Table 2, SI Table 2) has an effect on modelled carbon
250  dynamics in the organic layer, but this effect is strongly attenuated in the 0-5 cm layer in the mineral soil and
251  virtually absent for the deeper soil layers. The residual errors associated to the carbon turnover time estimates
252  converge to a single point (Figure 2) and are low (i.e. < 0.06 R, SI Tables 3 and 4). Turnover times show two
253  modes of behavior for well-drained soils and hydromorphic soils, respectively. The non-hydromorphic soils have
254  relatively similar values with decadal turnover times for the 0-5 cm layer, increasing to an order of centuries down

to 20 cm depth, and to millenia in deeper soil layers (~980 to ~3940 years at 0.6 to 1 m depth) (Fig. 5). In contrast, the hydromorphic soils are marked by turnover times that are up to an order of magnitude larger, from centennial in top soil to (multi-) millennial in deeper soils. At the Beatenberg Podzol, turnover time in the shallow layer which overlaps with the elluvial horizon is slower (20-40 cm, ~1900 y) than the deepest layer (40-60 cm, ~1300 y), which overlaps with the illuvial horizon (Figure 5, SI Table 5).

Carbon stocks also show distinct difference between drained and hydromorphic soils with greater stock in the hydromorphic soils (~15 kg C m$^{-2}$ at Beatenberg and Alptal vs. ~ 6 - ~7 kg C m$^{-2}$ at Othmarsingen, Lausanne and Nationalpark, Fig. 5, Table 3)).

The turnover times of the WEOC mimic the trends in the bulk soil but are up to an order of magnitude faster. Considering WEOC turnover time in the non-hydromorphic soils only, there is a slight increase in WEOC turnover time with decreasing site temperature, but the trend is not significant (SI Table 4). The modeled estimate for dynamic fraction is variable at the surface but decreases towards the lower top soil (from ~0.2 at 0-5 cm to ~0.01 at 10-20 cm in Othmarsingen). In the deep soil, the model indicates there could also be a non-negligible proportion of dynamic carbon (e.g. 0.10-0.23 at 20-40 cm). The residual errors associated to the error reduction of the two-pool model are also low (i.e. < 0.06 R). but do not converge as strongly as the single-pool model (SI Figure 1).

### 3.3 Pre-glacial carbon in deep soil profiles

The turnover times of deep soil carbon exceed 10,000 years in several profiles, indicating the presence of carbon that pre-dates the glacial retreat (Fig. 6). These profiles are located on carbon-containing bedrock and concern the deeper soil (80-100 cm) of the Gleysol (Alptal), as well as >100 cm in the Cambisol (Lausanne) (Fig. 6, SI Table 6).

### 3.4 Environmental drivers of carbon dynamics

Pearson correlation was used to assess potential relationships between carbon stocks and turnover time and their potential controlling factors (climate, NPP, soil texture, soil moisture and physicochemical properties (Table 4, SI Table 7, 8)). For the averaged top soil (0-20 cm, n=5), carbon stocks were significantly positive correlated to Mean Annual Precipitation (MAP). Turnover time in the bulk top soil negatively correlated with silt content and positively with average grain size. Turnover time in the WEOC of the top soil did not correlate significantly with any parameter except a weak positive correlation with grain size. Deeper soil bulk stock and turnover time positively correlated with MAP and iron content.

### 4 Discussion

### 4.1 Dynamic deep soil carbon

### 4.1.1 Rapid shifts in $^{14}$C abundance reflect dynamic deep carbon

The propagation of bomb-derived carbon into supposedly stable deep soil on the bulk level across the climatic gradient implies that SOM in deep soil contains a dynamic pool and could be less stable and potentially more vulnerable to change than previously thought. This possibility is further supported by the WEO$^{14}$C which is consistently more enriched in bomb-derived carbon than the bulk soil. Near-atmospheric signature WEO$^{14}$C

295    pervades up to 40 or even 60 cm depth. Hagedorn et al., (2004) also found WEOC to be a highly dynamic pool
296    using ^{13}C tracer experiments in forest soils.

297    We consider our ^{14}C comparison over time to be robust because the grid-based sampling and averaging was
298    repeated on the same plots which excludes the effect plot-scale variability (Van der Voort et al., 2016). Our [14]C
299    time-series data in the deep soil corroborate pronounced changes in [14]C (hence substantial SOM changes)
300    observed in subsoils of an area with pine afforestation (Richter and Markewitz, 2001). The findings are also in
301    agreement with results from an incubation study by Fontaine et al., (2007) which showed that the deep soil can
302    have a significant dynamic component. Baisden et al., (2007) also found indications of a deep dynamic pool using
303    modeling on ^{14}C time-series on the bulk level on a New Zealand soil under stable pastoral management.

304

### 305    4.1.2    Carbon dynamics reflect soil-specific characteristics at depth

306    Bulk carbon turnover time for the top and deeper soil fall in the range of prior observations and models, although
307    the data for the latter category is rare (Scharpenseel and Becker-Heidelmann, 1989; Paul et al., 1997; Schmidt et
308    al., 2011; Mills et al., 2013; Braakhekke et al., 2014). The carbon turnover time is related to soil-specific
309    characteristics. The higher turnover times of hydromorphic as compared to non-hydromorphic soils is likely due
310    to increased waterlogging and limited aerobicity (Hagedorn et al., 2001) which is conducive to slow
311    decomposition rates and enhanced carbon accumulation. The WEOC turns over up to an order of magnitude faster
312    than the bulk and mirrors these trends, indicating that it indeed is a more dynamic pool (Hagedorn et al., 2004;
313    Lechleitner et al., 2016). Results also reflect known horizon-specific dynamics for certain soil types, particularly
314    in the deep soil. The hydromorphic Podzol at Beatenberg shows specific pedogenetic features such as an
315    illuviation layer with an enrichment in humus and iron in the deeper soil (Walthert et al., 2003) where the turnover
316    time of bulk and WEOC is more rapid and stocks are higher as compared to the elluvial layer above (Fig. 5). This
317    is likely due to the input of younger carbon via leaching of dissolved organic carbon. The non-hydromorphic
318    Luvisols are marked by an enrichment of clay in the deeper soil, which can enhance carbon stabilization (Lutzow
319    et al., 2006). This also reflected in the turnover time of the 60-80 cm layer in the Othmarsingen Luvisol – in this
320    clay-enriched depth interval (Walthert et al., 2003), turnover time is relatively high as compared to the other
321    (colder) non-hydromorphic soils (Fig. 5). These patterns are consistent with findings by Mathieu et al., (2015)
322    that the important role of soil pedology on deep soil carbon dynamics.

323

### 324    4.1.3    Dynamic carbon at depth & implications for carbon transport

325    The analytical ^{14}C data as well as turnover time estimates indicate that there is likely a dynamic portion of carbon
326    in the deep soil. The estimated size of the dynamic pool can be large, even at greater depth than it was observed
327    by other ^{14}C time-series (Richter and Markewitz, 2001; Baisden and Parfitt, 2007; Koarashi et al., 2012). The two-
328    pool modelling indicates that the size of dynamic pool in the deep soil can be upwards of ~10%. A deep dynamic
329    pool is consistent with findings of a ^{13}C tracer experiment by Hagedorn et al., (2001) that shows with that relatively
330    young (<4 years) carbon can be rapidly incorporated in the top soil (20% new C at 0-20 cm depth) but also in the
331    deep soil (50 cm), and findings by Balesdent et al., (2018) which estimate that up to 21% of the carbon between
332    30-100 cm is younger than 50 years. Rumpel and Kögel-Knabner (2011) have highlighted the importance of the
333    poorly understood deep soil carbon stocks and a significant dynamic pool in the deep soil could imply that carbon
334    is more vulnerable than initially suspected. One major input pathway of younger C into deeper soils is the leaching

335 of DOC (Kaiser and Kalbitz, 2012; Sanderman and Amundson, 2009). Here, we have measured WEOC – likely
336 primarily composed of microbial metabolites (Hagedorn et al., 2004) – carrying a younger $^{14}C$ signature than bulk
337 SOM and thus, representing a translocator of fresh carbon to the deep soil. The WEOC turnover time is in the
338 order of decades, implying that it is not directly derived from decaying vegetation, but rather composed of
339 microbial material feeding on the labile portion of the bulk soil. In addition to WEOC, roots and associated
340 mycorrhizal communities may also provide a substantial input of new C into soils in deeper soils (Rasse et al.,
341 2005). Additional modelling such as in CENTURY and RotC could provide additional insights into the soil carbon
342 dynamics and fluxes (Manzoni et al., 2009)
343

344 **4.2     Contribution of petrogenic carbon**
345 Our results on deep soil carbon suggest the presence of pre-aged or $^{14}C$-dead (fossil), pre-interglacial carbon in
346 the Alptal (Gleysol) and Lausanne (Cambisol) profiles, implying that a component of soil carbon is not necessarily
347 linked to recent (< millenial) terrestrial productivity and instead constitutes part of the long-term (geological)
348 carbon cycle (> millions of years). In the case of the Gleysol in Alptal, the $^{14}C$-depleted material could be derived
349 from the poorly consolidated sedimentary rocks (Flysch) in the region (Hagedorn et al., 2001a; Schleppi et al.,
350 1998; Smith et al., 2013), whereas carbon present in glacial deposits and molasse may contribute in deeper soils
351 at the Lausanne (Cambisol) site. The potential contribution of fossil carbon was estimated using a mixing model
352 using the signature of a soil without fossil carbon, the signature of fossil carbon and the measured values (SI Table
353 4). Fossil carbon contribution in the Alptal profile between 80-100 cm (Fig. 6, SI Table 4) is estimated at ~40 %.
354 Below one meter at Lausanne site the petrogenic percentage ranges from ~20% at 145 cm up to ~80 % at 310 cm
355 depth (Fig. 6, SI Table 4).
356         Other studies analyzing soils have observed the significant presence of petrogenic (geogenic in soil
357 science terminology) in loess-based soils (Helfrich et al., 2007; Paul et al., 2001). Our results suggest that pre-
358 glacial carbon may comprise a dominant component of deep soil organic matter in several cases, resulting in an
359 apparent increase in the average turnover time of carbon in these soils. Hemingway et al., (2018) have highlighted
360 that fossil carbon oxidized in soils can lead to significant additional $CO_2$ emissions. Therefore, the potential of
361 soils to 'activate' fossil petrogenic carbon should be considered when evaluating the soil carbon sequestration
362 potential.
363

364 **4.3     Controls on carbon dynamics and cycling**
365 In order to examine the effects of potential controls on soil C turnover time and stocks, we explore correlations
366 between a number of available factors which have previously been proposed, such as texture, geology,
367 precipitation, temperature and soil moisture (Doetterl et al., 2015; McFarlane et al., 2013; Nussbaum et al., 2014;
368 Seneviratne et al., 2010; van der Voort et al., 2016).
369 From examination of data for all samples it emerges that C turnover time does not exhibit a consistent correlation
370 with any specific climatological or physico-chemical factor. This implies that no single mechanism predominates
371 and/or that there is a combined impact of geology and precipitation as these soil-forming factors affect grain size
372 distribution, water regime and mass transport in soils. Exploring potential relationships in greater detail, we see
373 that carbon stocks in the top soil and deep soil as well as turnover time is positively related to MAP, which could
374 be linked to waterlogging and anaerobic conditions even in upland soils leading to a lower decomposition and

thus to a higher build-up of organic material (Keiluweit et al., 2015). Our results are supported by the findings based on >1000 forest sites that precipitation exerts a strong effect on soil C stocks across Switzerland (Gosheva et al., 2017; Nussbaum et al., 2014). Furthermore, Balesdent et al., (2008) also highlighted the role of precipitation and evapotranspiration on deep soil organic carbon stabilisation. Nonetheless, it has to be noted that for these sites, the precipitation range does not include very dry soils (MAP 864-2126 mm/y). Topsoil carbon turnover time in bulk and WEOC positively correlates with grain size which is likely caused by the large grain size of the waterlogged Podzol Beatenberg. Overall, geology seems to impact the carbon cycling in three key ways. Firstly, when petrogenic carbon is present in the bedrock from shale or reworked shale (Schleppi et al., 1998; Walthert et al., 2003), fossil carbon contributes to soil carbon. Secondly, porosity of underlying bedrock either prevents or induces waterlogging which in turn affects turnover time. Thirdly, the initial components of the bedrock influence the final grain size distribution and mineralogy (SI Fig. 2, Table 3), which is also reflected in the carbon stock, bulk and pool-specific turnover time. Within the limited geographic and temporal scope of this paper, we hypothesize that for soil carbon stocks and their turnover time, temperature is not the dominant driver, which has been concluded by some (Giardina and Ryan, 2000) but refuted by others (Davidson et al., 2000; Feng et al., 2008). The only climate-related driver which appears to be significant for the deep soil is precipitation.

### 4.4 Modular robust numerical optimization

The numerical approach used here builds on previous work concerning turnover modeling of bomb-radiocarbon dominated samples (Herold et al., 2014; Solly et al., 2013; Torn et al., 2009) and the approach used in numerous time-series analysis with box modeling using Excel (Schrumpf and Kaiser, 2015) or Excel solver (Baisden et al., 2013; Prior et al., 2007). However certain modifications were made in order to (i) provide objective repeatable estimates, (ii) incorporate longer time-series data, and (iii) identify samples impacted by petrogenic (also called geogenic) carbon. Identifying petrogenic carbon in the deep soil is important considering the large carbon stocks in deep soils (Rumpel and Kogel-Knabner, 2011) and the wider relevance of petrogenically-derived carbon in the global carbon cycle (Galy et al., 2008). This approach is modular and could be adapted in the future to identify the correct turnover time for time-series ^{14}C data, which is becoming increasingly important with the falling bomb-peak (Graven, 2015). For the single and time-series data, the results from the numerical solution were benchmarked to the Excel-based model, and it was found that the results agree.

Other studies (e.g. Baisden and Canessa, 2012; Prior et al., 2007) also use time-series data to estimate the value for two unknowns simultaneously (size of the pool size and turnover time). The error does not always converge to single low point, but can have multiple minima (SI Fig. 1). This potential issue should be considered when interpreting the data. More time-series data is required to eliminate this problem.

### 5 Conclusion

Time-series radiocarbon (^{14}C) analyses of soil carbon across a climatic range reveals recent bomb-derived radiocarbon in both upper and deeper bulk soil, implying the presence of a rapidly turning over pool at depth. Pool-specific time-series measurements of the WEOC indicate this is a more dynamic pool which is consistently more enriched in radiocarbon than the bulk. Furthermore, the estimated modeled size of the dynamic fraction is non-negligible even in the deep soil (~0.1-0.2). This could imply that a component of the deep soil carbon could be more dynamic than previously thought.

415    The interaction between precipitation and geology appears to be the main control on carbon dynamics
416    rather than site temperature. Carbon turnover time in non-hydromorphic soils is relatively similar (decades to
417    centuries) despite dissimilar climatological conditions. Hydromorphic soils have turnover times which are up to
418    an order of magnitude slower. These trends are mirrored in the dynamic WEOC pool, suggesting that in non-
419    waterlogged (aerobic) soils the transport of relatively modern (bomb-derived) carbon into the deep soil and/or the
420    microbial processing is enhanced as compared to waterlogged (anaerobic) soils.

421    Model results indicate certain soils contain significant quantities of pre-glacial or petrogenic (bedrock-
422    derived) carbon in the deeper part of their profiles. This implies that soils not only sequester "modern" but can
423    rather also mobilize and potentially metabolize "fossil" or geogenic carbon.

424    Overall, these time-series $^{14}$C bulk and pool-specific data provide novel constraints on soil carbon
425    dynamics in surface and deeper soils for a range of ecosystems.

426

**Acknowledgements**

We would like to acknowledge the SNF NRP68 *Soil as a Resource* program for funding this project (SNF 406840_143023/11.1.13-31.12.15). We could also like to thank Jerome Balesdent, an anonymous reviewer and the journal editor Sébastian Fontaine for their helpful comments from which this paper greatly benefitted. We would like to thank various members of the Laboratory of Ion Beam Physics and Biogeoscience group for their help with the analyses, in particular Lukas Wacker. We thank Roger Köchli for his crucial help in the field which enabled an effective time-series comparison and for his help with subsequent analyses. We thank Emily Solly and Sia Gosheva for their valuable insights, Claudia Zell for her help on the project and in the field, Peter Waldner and Marco Walser for facilitating the fieldwork, and Elisabeth Graf-Pannatier for her insights on soil moisture. The 2014 field campaign would not have been possible without the help of Thomas Blattmann, Lukas Oesch, Markus Vaas and Niko Westphal. Thanks to Stephane Beaussier for the insights into numerical modeling. Also thanks to Nadine Keller and Florian Neugebauer for their help in the lab. Last but not least, thanks to Thomas Bär for summarizing ancillary pH data. Data supporting this paper is provided in a separate data Table. All soil samples used in this study are stored in the long-term soil storage facility of the Swiss Federal Institute of Forest, Snow and Landscape Research (WSL).

**References**

Angst, G., John, S., Mueller, C. W., Kögel-Knabner, I. and Rethemeyer, J.: Tracing the sources and spatial distribution of organic carbon in subsoils using a multi-biomarker approach, Sci. Rep., 6(1), 29478, doi:10.1038/srep29478, 2016.

Von Arx, G., Graf Pannatier, E., Thimonier, A. and Rebetez, M.: Microclimate in forests with varying leaf area index and soil moisture: Potential implications for seedling establishment in a changing climate, J. Ecol., 101(5), 1201–1213, doi:10.1111/1365-2745.12121, 2013.

Baisden, W. T. and Parfitt, R. L.: Bomb 14C enrichment indicates decadal C pool in deep soil?, Biogeochemistry, 85(1), 59–68, doi:10.1007/s10533-007-9101-7, 2007.

Baisden, W. T., Parfitt, R. L., Ross, C., Schipper, L. A. and Canessa, S.: Evaluating 50 years of time-series soil radiocarbon data : towards routine calculation of robust C residence times, Biogeochemistry, 112, 129–137, doi:10.1007/s10533-011-9675-y, 2013.

Batjes, N. H.: Total carbon and nitrogen in the soils of the world, Eur. J. Soil Sci., 47(June), 151–163, 1996.

Balesdent, J., Basile-Doelsch, I., Chadoeuf, J., Cornu, S., Derrien, D., Fekiacova, Z. and Hatté, C.: Atmosphere–soil carbon transfer as a function of soil depth, Nature, 559(7715), 599–602, doi:10.1038/s41586-018-0328-3, 2018.

Braakhekke, M. C., Beer, C., Schrumpf, M., Ekici, A., Ahrens, B., Hoosbeek, M. R., Kruijt, B., Kabat, P. and Reichstein, M.: The use of radiocarbon to constrain current and future soil organic matter turnover and transport in a temperate forest, J. Geophys. Res. Biogeosciences, 119(3), 372–391, doi:10.1002/2013JG002420, 2014.

Carvalhais, N., Forkel, M., Khomik, M., Bellarby, J., Jung, M., Migliavacca, M., Mu, M., Saatchi, S., Santoro, M., Thurner, M., Weber, U., Ahrens, B., Beer, C., Cescatti, A., Randerson, J. T., Reichstein, M., Mu, M., Saatchi, S., Santoro, M., Thurner, M., Weber, U., Ahrens, B., Beer, C., Cescatti, A., Randerson, J. T., Reichstein, M., Mu, M., Saatchi, S., Santoro, M., Thurner, M., Weber, U., Ahrens, B., Beer, C., Cescatti, A., Randerson, J. T. and Reichstein, M.: Global covariation of carbon turnover times with climate in terrestrial ecosystems, Nature, 514(7521), 213–217, doi:10.1038/nature13731, 2014.

Crowther, T., Todd-Brown, K., Rowe, C., Wieder, W., Carey, J., Machmuller, M., Snoek, L., Fang, S., Zhou, G., Allison, S., Blair, J., Bridgham, S., Burton, A., Carrillo, Y., Reich, P., Clark, J., Classen, A., Dijkstra, F., Elberling, B., Emmett, B., Estiarte, M., Frey, S., Guo, J., Harte, J., Jiang, L., Johnson, B., Kröel-Dulay, G., Larsen, K., Laudon, H., Lavallee, J., Luo, Y., Lupascu, M., Ma, L., Marhan, S., Michelsen, A., Mohan, J., Niu, S., Pendall, E., Penuelas, J., Pfeifer-Meister, L., Poll, C., Reinsch, S., Reynolds, L., Schmidth, I., Sistla, S., Sokol, N., Templer, P., Treseder, K., Welker, J. and Bradford, M.: Quantifying global soil C losses in response to warming, Nature, 540(1), 104–108, doi:10.1038/nature20150, 2016.

Davidson, E. A. and Janssens, I. A.: Temperature sensitivity of soil carbon decomposition and feedbacks to climate change., Nature, 440(7081), 165–73 [online] Available from: http://www.ncbi.nlm.nih.gov/pubmed/16525463 (Accessed 28 May 2014), 2006.

Davidson, E. A., Trumbore, S. E. and Amundson, R.: Soil warming and organic carbon content., Nature,

479     408(December), 789–790, doi:10.1038/35048672, 2000.
480     Doetterl, S., Stevens, A., Six, J., Merckx, R., Oost, K. Van, Pinto, M. C., Casanova-katny, A., Muñoz, C.,
481     Boudin, M., Venegas, E. Z. and Boeckx, P.: Soil carbon storage controlled by interactions between
482     geochemistry and climate, Nat. Geosci., 8(August), 1–4, doi:10.1038/NGEO2516, 2015.
483     Etzold, S., Waldner, P., Thimonier, A., Schmitt, M. and Dobbertin, M.: Tree growth in Swiss forests between
484     1995 and 2010 in relation to climate and stand conditions: Recent disturbances matter, For. Ecol. Manage., 311,
485     41–55 [online] Available from: http://linkinghub.elsevier.com/retrieve/pii/S0378112713003393 (Accessed 3
486     June 2014), 2014.
487     Feng, X., Simpson, A. J., Wilson, K. P., Williams, D. D. and Simpson, M. J.: Increased cuticular carbon
488     sequestration and lignin oxidation in response to soil warming, Nat. Geosci., 1(December), 836–839, 2008.
489     Fierer, N., Schimel, J. P. and Holden, P. A.: Variations in microbial community composition through two soil
490     depth profiles, Soil Biol. Biochem., 35, 167–176, 2003.
491     Fontaine, S., Barot, S., Barré, P., Bdioui, N., Mary, B. and Rumpel, C.: Stability of organic carbon in deep soil
492     layers controlled by fresh carbon supply., Nature, 450, 277–280, 2007.
493     Fröberg, M., Tipping, E., Stendahl, J., Clarke, N. and Bryant, C.: Mean residence time of O horizon carbon
494     along a climatic gradient in Scandinavia estimated by 14C measurements of archived soils, Biogeochemistry,
495     104(1–3), 227–236 [online] Available from: http://link.springer.com/10.1007/s10533-010-9497-3 (Accessed 2
496     August 2013), 2010.
497     Galy, V., Beyssac, O., France-Lanord, C. and Eglinton, T. I.: Recycling of graphite during Himalayan erosion: a
498     geological stabilization of carbon in the crust, Science (80-. )., 322(November), 943–945,
499     doi:10.1126/science.1161408, 2008.
500     Giardina, C. P. and Ryan, M. G.: Evidence that decomposition rates of organic carbon in mineral soil do not
501     vary with temperature, Nature, 404(6780), 858–861, doi:10.1038/35009076, 2000.
502     Gosheva, S., Walthert, L., Niklaus, P. A., Zimmermann, S., Gimmi, U. and Hagedorn, F.: Reconstruction of
503     Historic Forest Cover Changes Indicates Minor Effects on Carbon Stocks in Swiss Forest Soils, Ecosystems,
504     (C), doi:10.1007/s10021-017-0129-9, 2017.
505     Graven, H. D.: Impact of fossil fuel emissions on atmospheric radiocarbon and various applications of
506     radiocarbon over this century, Proc. Natl. Acad. Sci., (Early Edition), 1–4, doi:10.1073/pnas.1504467112,
507     2015a.
508     Graven, H. D.: Impact of fossil fuel emissions on atmospheric radiocarbon and various applications of
509     radiocarbon over this century, Proc. Natl. Acad. Sci., (Early Edition), 1–4, doi:10.1073/pnas.1504467112,
510     2015b.
511     Hagedorn, F., Bucher, J. B. and Schleppi, P.: Contrasting dynamics of dissolved inorganic and organic nitrogen
512     in soil and surface waters of forested catchments with Gleysols, Geoderma, 100(1–2), 173–192,
513     doi:10.1016/S0016-7061(00)00085-9, 2001a.
514     Hagedorn, F., Maurer, S., Egli, P., Blaser, P., Bucher, J. B. and Siegwo: Carbon sequestration in forest soils :
515     effects of soil type , atmospheric CO 2 enrichment , and N deposition, Eur. J. Soil Sci., 52(December), 2001b.
516     Hagedorn, F., Saurer, M. and Blaser, P.: A 13C tracer study to identify the origin of dissolved organic carbon in
517     forested mineral soils, Eur. J. Soil Sci., 55(1), 91–100 [online] Available from:
518     http://doi.wiley.com/10.1046/j.1365-2389.2003.00578.x (Accessed 26 September 2013), 2004.
519     He, Y., Trumbore, S. E., Torn, M. S., Harden, J. W., Vaughn, L. J. S., Allison, S. D. and Randerson, J. T.:
520     Radiocarbon constraints imply reduced carbon uptake by soils during the 21st century, Science (80-. ).,
521     353(6306), 1419–1424, 2016.
522     Helfrich, M., Flessa, H., Mikutta, R., Dreves, A. and Ludwig, B.: Comparison of chemical fractionation
523     methods for isolating stable soil organic carbon pools, Eur. J. Soil Sci., 58(6), 1316–1329, doi:10.1111/j.1365-
524     2389.2007.00926.x, 2007.
525     Hemingway, J.: Microbial oxidation of lithospheric organic carbon in rapidly eroding tropical mountain soils,
526     Science (80-. )., (April), doi:10.1126/science.aao6463, 2018.
527     Herold, N., Schöning, I., Michalzik, B., Trumbore, S. E. and Schrumpf, M.: Controls on soil carbon storage and
528     turnover in German landscapes, Biogeochemistry, 119(1–3), 435–451, doi:x, 2014.
529     Hua, Q., Barbetti, M. and Rakowski, A. Z.: Atmospheric radiocarbon for the period 1950–2010, Radiocarbon,
530     55(4), 2059–2072, 2013.
531     Ivy-Ochs, S., Kerschner, H., Maisch, M., Christl, M., Kubik, P. W. and Schluchter, C.: Latest Pleistocene and
532     Holocene glacier variations in the European Alps, Quat. Sci. Rev., 28(21–22), 2137–2149,
533     doi:10.1016/j.quascirev.2009.03.009, 2009.
534     Jobbagy, E. G. and Jackson, R. .: Ther vertical distribution of soil organic carbon an its relation to climate and
535     vegetation, Ecol. Appl., 10(April), 423–436, 2000.
536     Kaiser, K. and Kalbitz, K.: Cycling downwards - dissolved organic matter in soils, Soil Biol. Biochem., 52, 29–
537     32, doi:10.1016/j.soilbio.2012.04.002, 2012.
538     Keiluweit, M., Bougoure, J. J., Nico, P. S., Pett-Ridge, J., Weber, P. K. and Kleber, M.: Mineral protection of

539    soil carbon counteracted by root exudates, Nat. Clim. Chang., 5(6), doi:10.1038/nclimate2580, 2015.

540    Klute, A.: Methods of soil analysis, Part 1: Physical and Mineralogical Methods, 2nd ed., Agronomy
541    Monograph No 9, Madison WI., 1986.

542    Koarashi, J., Hockaday, W. C., Masiello, C. a. and Trumbore, S. E.: Dynamics of decadally cycling carbon in
543    subsurface soils, J. Geophys. Res. Biogeosciences, 117(3), 1–13, doi:10.1029/2012JG002034, 2012.

544    Komada, T., Anderson, M. R. and Dorfmeier, C. L.: Carbonate removal from coastal sediments for the
545    determination of organic carbon and its isotopic signatures , δ 13 C and Δ 14 C : comparison of fumigation and
546    direct acidification by hydrochloric acid, Limnol. Oceanogr. Methods, (6), 254–262, 2008.

547    Lang, S. Q., McIntyre, C. P., Bernasconi, S. M., Früh-Green, G. L., Voss, B. M., Eglinton, T. I. and Wacker, L.:
548    Rapid 14C Analysis of Dissolved Organic Carbon in Non-Saline Waters, Radiocarbon, 58(3), 1–11,
549    doi:10.1017/RDC.2016.17, 2016.

550    Lechleitner, F. A., Baldini, J. U. L., Breitenbach, S. F. M., Fohlmeister, J., McIntyre, C., Goswami, B.,
551    Jamieson, R. A., van der Voort, T. S., Prufer, K., Marwan, N., Culleton, B. J., Kennett, D. J., Asmerom, Y.,
552    Polyak, V. and Eglinton, T. I.: Hydrological and climatological controls on radiocarbon concentrations in a
553    tropical stalagmite, Geochim. Cosmochim. Acta, doi:10.1016/j.gca.2016.08.039, 2016.

554    Lutzow, M. V, Kogel-Knabner, I., Ekschmitt, K., Matzner, E., Guggenberger, G., Marschner, B. and Flessa, H.:
555    Stabilization of organic matter in temperate soils: mechanisms and their relevance under different soil
556    conditions - a review, Eur. J. Soil Sci., 57, 426–445 [online] Available from:
557    http://doi.wiley.com/10.1111/j.1365-2389.2006.00809.x, 2006.

558    McFarlane, K. J., Torn, M. S., Hanson, P. J., Porras, R. C., Swanston, C. W., Callaham, M. A. and Guilderson,
559    T. P.: Comparison of soil organic matter dynamics at five temperate deciduous forests with physical
560    fractionation and radiocarbon measurements, Biogeochemistry, 112(1–3), 457–476, doi:10.1007/s10533-012-
561    9740-1, 2013.

562    Manzoni, S., Katul, G. G. and Porporato, A.: Analysis of soil carbon transit times and age distributions using
563    network theories, J. Geophys. Res. Biogeosciences, 114(4), 1–14, doi:10.1029/2009JG001070, 2009.

564    Mathieu, J. A., Hatté, C., Balesdent, J. and Parent, É.: Deep soil carbon dynamics are driven more by soil type
565    than by climate: A worldwide meta-analysis of radiocarbon profiles, Glob. Chang. Biol., 21(11), 4278–4292,
566    doi:10.1111/gcb.13012, 2015.

567    McIntyre, C. P., Wacker, L., Haghipour, N., Blattmann, T. M., Fahrni, S., Usman, M., Eglinton, T. I. and Synal,
568    H.-A.: Online 13C and 14C Gas Measurements by EA-IRMS–AMS at ETH Zürich, Radiocarbon,
569    002(November 2015), 1–11, doi:10.1017/RDC.2016.68, 2016.

570    Melillo, J. M., Steudler, P. a, Aber, J. D., Newkirk, K., Lux, H., Bowles, F. P., Catricala, C., Magill, A., Ahrens,
571    T. and Morrisseau, S.: Soil warming and carbon-cycle feedbacks to the climate system., Science, 298(5601),
572    2173–6 [online] Available from: http://www.ncbi.nlm.nih.gov/pubmed/12481133 (Accessed 21 January 2014),
573    2002.

574    Mills, R. T. E., Tipping, E., Bryant, C. L. and Emmett, B. a.: Long-term organic carbon turnover rates in natural
575    and semi-natural topsoils, Biogeochemistry, 118(1), 257–272 [online] Available from:
576    http://link.springer.com/10.1007/s10533-013-9928-z (Accessed 18 December 2013a), 2013.

577    Mills, R. T. E., Tipping, E., Bryant, C. L. and Emmett, B. a.: Long-term organic carbon turnover rates in natural
578    and semi-natural topsoils, Biogeochemistry, 118(1), 257–272 [online] Available from:
579    http://link.springer.com/10.1007/s10533-013-9928-z, 2013b.

580    Nussbaum, M., Papritz, A., Baltensweiler, A. and Walthert, L.: Estimating soil organic carbon stocks of Swiss
581    forest soils by robust external-drift kriging, Geosci. Model Dev., 7(3), 1197–1210, doi:10.5194/gmd-7-1197-
582    2014, 2014.

583    Paul, E. A., Collins, H. P. and Leavitt, S. W.: Dynamics of resistant soil carbon of midwestern agricultural soils
584    measured by naturally occurring 14C abundance, Geoderma, 104(3–4), 239–256, doi:10.1016/S0016-
585    7061(01)00083-0, 2001.

586    Paul, E. A., Follett, R. F., Leavitt, W. S., Halvorson, A., Petersen, G. A. and Lyon, D. J.: Radiocarbon Dating
587    for Determination of Soil Organic Matter Pool Sizes and Dynamics, Soil Sci. Soc. Am. J., 61(4), 1058–1067,
588    1997.

589    Prietzel, J., Zimmermann, L., Schubert, A. and Christophel, D.: Organic matter losses in German Alps forest
590    soils since the 1970s most likely caused by warming, Nat. Geosci., 9(July), doi:10.1038/ngeo2732, 2016.

591    Prior, C. A., Baisden, W. T., Bruhn, F. and Neff, J. C.: Using a soil chronosequence to identify soil fractions for
592    understanding and modeling soil carbon dynamics in New Zealand, Radiocarbon, 49(2), 1093–1102, 2007.

593    Rasse, D. P., Rumpel, C. and Dignac, M.-F.: Is soil carbon mostly root carbon? Mechanisms for a specific
594    stabilisation, Plant Soil, 269(1–2), 341–356 [online] Available from: http://link.springer.com/10.1007/s11104-
595    004-0907-y, 2005.

596    Rethemeyer, J., Kramer, C., Gleixner, G., John, B., Yamashita, T., Flessa, H., Andersen, N., Nadeau, M. and
597    Grootes, P. M.: Transformation of organic matter in agricultural soils : radiocarbon concentration versus soil
598    depth, Geoderma, 128, 94–105, doi:10.1016/j.geoderma.2004.12.017, 2005.

599    Richter, D. D. and Markewitz, D.: Understanding Soil Change, Cambridge University Press, Cambridge., 2001.

600    Rumpel, C. and Kogel-Knabner, I.: Deep soil organic matter—a key but poorly understood component of

601    terrestrial C cycle, Plant Soil, 338, 143–158, 2011a.

602    Rumpel, C. and Kogel-Knabner, I.: Deep soil organic matter—a key but poorly understood component of

603    terrestrial C cycle, Plant Soil, 338, 143–158, 2011b.

604    Sanderman, J. and Amundson, R.: A comparative study of dissolved organic carbon transport and stabilization

605    in California forest and grassland soils, Biogeochemistry, 92(1–2), 41–59, doi:10.1007/s10533-008-9249-9,

606    2009.

607    Scharpenseel, H. W. and Becker-Heidelmann, P.: Shifts in 14C patterns of soil profiles due to bomb carbon,

608    including effects of morphogenetic and turbation processes, Radiocarbon, 31(3), 627–636, 1989.

609    Schaub, M., Dobbertin, M., Kräuchi, N. and Dobbertin, M. K.: Preface-long-term ecosystem research:

610    Understanding the present to shape the future, Environ. Monit. Assess., 174(1–4), 1–2, doi:10.1007/s10661-010-

611    1756-1, 2011.

612    Schimel, D. S., House, J. I., Hibbard, K. a, Bousquet, P., Ciais, P., Peylin, P., Braswell, B. H., Apps, M. J.,

613    Baker, D., Bondeau, A., Canadell, J., Churkina, G., Cramer, W., Denning,  a S., Field, C. B., Friedlingstein, P.,

614    Goodale, C., Heimann, M., Houghton, R. a, Melillo, J. M., Moore, B., Murdiyarso, D., Noble, I., Pacala, S. W.,

615    Prentice, I. C., Raupach, M. R., Rayner, P. J., Scholes, R. J., Steffen, W. L. and Wirth, C.: Recent patterns and

616    mechanisms of carbon exchange by terrestrial ecosystems., Nature, 414(6860), 169–72 [online] Available from:

617    http://www.ncbi.nlm.nih.gov/pubmed/11700548, 2001.

618    Schleppi, P., Muller, N., Feyen, H., Papritz, A., Bucher, J. B. and Fluehler, H.: Nitrogen budgets of two small

619    experimental forested catchments at Alptal , Switzerland, For. Ecol. Manage., 127(101), 177–185, 1998.

620    Schmidt, M. W. I., Torn, M. S., Abiven, S., Dittmar, T., Guggenberger, G., Janssens, I. a, Kleber, M., Kögel-

621    Knabner, I., Lehmann, J., Manning, D. a C., Nannipieri, P., Rasse, D. P., Weiner, S. and Trumbore, S. E.:

622    Persistence of soil organic matter as an ecosystem property., Nature, 478(7367), 49–56 [online] Available from:

623    http://www.ncbi.nlm.nih.gov/pubmed/21979045 (Accessed 21 January 2014), 2011.

624    Schrumpf, M. and Kaiser, K.: Large differences in estimates of soil organic carbon turnover in density fractions

625    by using single and repeated radiocarbon inventories, Geoderma, 239–240, 168–178 [online] Available from:

626    http://linkinghub.elsevier.com/retrieve/pii/S0016706114003577, 2015.

627    Schrumpf, M., Kaiser, K., Guggenberger, G., Persson, T., Kogel-Knabner, I. and Schulze, E.-D.: Storage and

628    stability of organic carbon in soils as related to depth , occlusion within aggregates , and attachment to minerals,

629    Biogeosciences, 10, 1675–1691, 2013.

630    Seneviratne, S. I., Corti, T., Davin, E. L., Hirschi, M., Jaeger, E. B., Lehner, I., Orlowsky, B. and Teuling, A. J.:

631    Investigating soil moisture-climate interactions in a changing climate: A review, Earth-Science Rev., 99(3–4),

632    125–161, doi:10.1016/j.earscirev.2010.02.004, 2010.

633    Sierra, C. A., Muller, M., Metzler, H., Manzoni, S. and Trumbore, S. E.: The muddle of ages, turnover, transit,

634    and residence times in the carbon cycle, Glob. Chang. Biol., 1–11, doi:10.1111/gcb.13556, 2016.

635    Smith, J. C., Galy, A., Hovius, N., Tye, A. M., Turowski, J. M. and Schleppi, P.: Runoff-driven export of

636    particulate organic carbon from soil in temperate forested uplands, Earth Planet. Sci. Lett., 365, 198–208,

637    doi:10.1016/j.epsl.2013.01.027, 2013.

638    Solly, E., Schöning, I., Boch, S., Müller, J., Socher, S. a., Trumbore, S. E. and Schrumpf, M.: Mean age of

639    carbon in fine roots from temperate forests and grasslands with different management, Biogeosciences, 10(7),

640    4833–4843, doi:10.5194/bg-10-4833-2013, 2013.

641    Torn, M. S., Swanston, C. W., Castanha, C. and Trumbore, S. E.: Storage and turnover of organic matter in soil,

642    in Biophysico-Chemical Processes Involving Natural Nonliving Organic Matter in Environmental Systems,

643    edited by N. Senesi, B. Xing, and P. M. Huang, p. 54, John Wiley & Sons, Inc., 2009.

644    Trumbore, S. E. and Czimczik, C. I.: Geology. An uncertain future for soil carbon., Science, 321, 1455–1456,

645    2008.

646    van der Voort, T. S., Hagedorn, F., Mcintyre, C., Zell, C., Walthert, L. and Schleppi, P.: Variability in 14 C

647    contents of soil organic matter at the plot and regional scale across climatic and geologic gradients,

648    Biogeosciences, 13(January), 3427–3439, doi:10.5194/bg-2015-649, 2016.

649    Wacker, L., Bonani, G., Friedrich, M., Hajdas, I., Kromer, B., NÏmec, M., Ruff, M., Suter, M., Synal, H.-A. and

650    Vockenhuber, C.: MICADAS: Routine and high-precision radiocarbon dating, Radiocarbon, 52(2), 252–262,

651    2010.

652    Wacker, L., Němec, M. and Bourquin, J.: A revolutionary graphitisation system: Fully automated, compact and

653    simple, Nucl. Instruments Methods Phys. Res. Sect. B Beam Interact. with Mater. Atoms, 268(7–8), 931–934

654    [online] Available from: http://linkinghub.elsevier.com/retrieve/pii/S0168583X09011161 (Accessed 2 August

655    2013), 2009.

656    Walthert, L., Blaser, P., Lüscher, P., Luster, J. and Zimmermann, S.: Langfristige Waldökosystem-Forschung

657    LWF in der Schweiz. Kernprojekt Bodenmatrix. Ergebnisse der ersten Erhebung 1994–1999., 2003.

658    Walthert, L., Graf Pannatier, E. and Meier, E. S.: Shortage of nutrients and excess of toxic elements in soils

659    limit the distribution of soil-sensitive tree species in temperate forests, For. Ecol. Manage., 297, 94–107,
660    doi:10.1016/j.foreco.2013.02.008, 2013.
661    Walthert, L., Lüscher, P., Luster, J. and Peter, B.: Langfristige Waldökosystem- Forschung LWF. Kernprojekt
662    Bodenmatrix. Aufnahmeanleitung zur ersten Erhebung 1994–1999, Swiss Federal Institute for Forest, Snow and
663    Landscape Research WSL, Birmensdorf., 2002a.
664    Walthert, L., Lüscher, P., Luster, J. and Peter, B.: Langfristige Waldökosystem-Forschung LWF in der Schweiz.
665    Kernprojekt Bodenmatrix. Aufnahmeanleitung zur ersten Erhebung 1994–1999, Birmensdorf. [online]
666    Available from: http://e-collection.ethbib.ethz.ch/show?type=bericht&nr=269, 2002b.

667
668
669

670 **Author contributions**

671 T.S. van der Voort planned, coordinated and executed the sampling strategy and sample collection, performed the

672 analyses, conceptualized and optimized the model and processed resulting data. U. Mannu led the model

673 development. F. Hagedorn lent his expertise on soil carbon cycling and soil properties. C. McIntyre facilitated

674 and coordinated the radiocarbon measurements and associated data corrections. L. Walthert and P. Schleppi lent

675 their expertise on the legacy sampling and provided data for the compositional analysis. N. Haghipour performed

676 in isotopic and compositional measurements. T. Eglinton provided the conceptual framework and aided in the

677 paper structure set-up. T.S. van der Voort prepared the manuscript with help of all co-authors.

**Tables**

**Table 1** Overview sampling locations and climatic and ecological parameters.

| Location | Soil type | Geology | Latitude(N)/ Longitude (E) | Soil depth (m) | Depth Upper limit waterlogging (m)[1] | Altitude Elevation (m a.s.l.) | MAT °C | MAP mm y$^{-1}$ | NPP g C m$^{-2}$y$^{-1}$ |
|----------|-----------|---------|------------------------------|----------------|----------------------------------------|-------------------------------|--------|------------------|--------------------------|
| Othmarsingen[1, 2, 3] | Luvisol | Calcareous moraine | 47°24'/8°14' | >1.9 | 2.5 | 467-500 | 9.2 | 1024 | 845 |
| Lausanne[1, 2, 3] | Cambisol | Calcarous and shaly moraine | 46°34'/6°39' | >3.2 | 2.5 | 800-814 | 7.6 | 1134 | 824 |
| Alptal[1, 2, 3, 4] | Gleysol | Flysch (carbon-holding sedimentary rock) | 47°02'/8°43' | >1.0 | 0.1 | 1200 | 5.3 | 2126 | 347 |
| Beatenberg[1, 2, 3] | Podzol | Sandstone | 46°42'/7°46' | 0.65 | 0.5 | 1178-1191 | 4.7 | 1163 | 302 |
| Nationalpark[1, 2, 3] | Fluvisol | Calcareous alluvial fan | 46°40'/10°14' | >1.1 | 2.5 | 1890-1907 | 1.3 | 864 | 111 |

[1] Walthert et al. (2003) [2]Etzold et al., (2014) [3]Von Arx et al., (2013) [4]Krause et al., (2013) for Alptal data

**Table 2** Vegetation and soil data of the study sites. Soil water potential (hPa) are for 15 cm depth.

| Location[1] | Deciduous tree species (%)[3] | Dominant tree species[3] | Inferred lag carbon fixation (y) | Organic layer Type[1] | Soil water potential (hPa) percentiles[3] | | |
|---|---|---|---|---|---|---|---|
| | | | | | 5% | 50% | 95% |
| Othmarsingen | 100 | *Fagus sylvatica* | 2 | Mull | -577 | -39 | -9 |
| Lausanne | 80 | *Fagus sylvatica* | 3 | Mull | -547 | -49 | -8 |
| Alptal[4] | 15 | *Picea abies* | 7 | Mor to anmoor | -38 | -13 | +1 |
| Beatenberg | 0 | *Picea abies* | 8 | Mor | -50 | -14 | +1 |
| Nationalpark | 0 | *Pinus montana* | 8 | Moder | -388 | -65 | -13 |

[1] Walthert et al. (2003) [2] Etzold et al., (2014), [3] Von Arx et al. (2013), [4] Krause et al., (2013)

**Table 3** Soil properties as well as carbon stocks and fluxes in 0-20, 20-60, and 60-100 cm depth of the study sites for the bulk and water-extractable organic carbon (WEOC).

| Location | Depth interval (m) | pH[1] | CEC[1](mmolc/kg) | Fe$_{exchangeable}$ (mmolc/kg) | Al$_{exchangeable}$ (mmolc/kg) | Sand content (%) | Silt content (%) | Clay content (%) | Carbon stock kgC/m$^2$ | Average turnover time bulk (y) | Average turnover time WEOC (y) |
|---|---|---|---|---|---|---|---|---|---|---|---|
| Othmarsingen[1] | 0.0-0.2 | 4.4 | 62.2 | 0.15 | 42 | 46.8 | 35.5 | 17.6 | 4.84 | 173 | 35 |
| | 0.2-0.6 | 4.4 | 62.8 | 0.10 | 49 | 44.3 | 33.3 | 22.4 | 1.69 | 868 | 518 |
| | 0.6-0.8 | 4.9 | 99.5 | 0.06 | 41 | 46.7 | 28.4 | 25.0 | 0.28 | 3938 | - |
| Lausanne[1] | 0.0-0.2 | 4.5 | 60.8 | 0.13 | 43 | 49.2 | 32.6 | 18.2 | 3.24 | 353 | 77 |
| | 0.2-0.6 | 4.6 | 43.9 | 0 | 34 | 50.2 | 32.0 | 17.8 | 2.12 | 1239 | 588 |
| | 0.6-1.0 | 4.8 | 49.7 | 0 | 35 | 50.5 | 31.5 | 18.1 | 0.69 | 2246 | 1502[5] |
| Alptal[2,3,4] | 0.0-0.2 | 4.5 | 417 | - | 19 | 19.3 | 39.4 | 41.3 | 7.73 | 437 | 162 |
| | 0.2-0.6 | 4.7 | 340 | - | 14 | 4.90 | 47.0 | 48.1 | 7.24 | 3314 | 893[6] |
| | 0.6-1.0 | 4.7 | 340 | - | - | - | - | - | 6.54 | 5165 | - |
| Beatenberg[1] | Organic layer | 3.1 | 260.2 | 2.8 | 33 | - | - | - | 7.05 | 53 | - |
| | 0.0-0.2 | 4.0 | 35.6 | 1.7 | 18 | 84.9 | 12.4 | 2.7 | 3.65 | 1224 | 293 |
| | 0.2-0.6 | 4.1 | 23.1 | 0.40 | 17 | 83.2 | 12.3 | 4.6 | 4.10 | 1607 | 677 |
| Nationalpark[1] | 0.0-0.2 | 8.3 | 171.8 | 0.1 | 0.0 | 47.5 | 34.8 | 17.7 | 3.23 | 180 | 92 |
| | 0.2-0.6 | 8.8 | 106.3 | 0.0 | 0.0 | 61.9 | 32.5 | 5.7 | 0.36 | 612 | 214 |
| | 0.6-0.8 | - | - | 0.0 | 0.0 | 60.6 | 33.6 | 5.9 | 0.08 | 983 | - |

[1]Walthert et al., 2002, Walthert et al., 2003., Fe and Al content (mmolc/kg) determined by NH$_4$Cl extraction.

For the 0.2-0.6 depth interval the CEC determined for 0.2-0.4 m was taken, and similarly for the depth interval 0.6-1.0 m the values for 0.6-0.8 m were taken in the case of Othmarsingen, Lausanne Beatenberg and Nationalpark.

[2]Krause et al., 2013

[3]Diserens et al,1992, CEC determined (mmeq/kg), hydrogen lead and zinc ions were not included, Aluminium content determined by Lakanen method. CEC values for 0.2-0.4 m were extrapolated to 1 m. [4]Xu et al., 2009 [5]Depth to 0.8 m [6]Depth to 0.4 m

Table 4 Pearson correlations for averaged depth intervals for the top soil (0-20 cm, n=5) and deep soil (20-60 cm, n=5). Significance denoted with ˙, *, ** or *** for respectively p-values smaller than 0.1 (marginally significant) 0.05, 0.005 and 0.0005 (significant). Non-significant correlations are indicated by the superscript **ns**. SWP or soil water potential used are the median values at 15 cm for each of these 5 sites (Von Arx et al., 2013). Water-extractable carbon is abbreviated to WEOC. Results indicate that no single climatic or textural factor consistently co-varies with carbon stocks, or turnover time.

| Explaining variable | Stock$_{0\text{-}20\ cm}$ | Turnover time bulk$_{0\text{-}20\ cm}$ | Turnover time WEOC $_{0\text{-}20\ cm}$ | Stock$_{20\text{-}60\ cm}$ | Turnover time$_{20\text{-}60\ cm}$ |
|---|---|---|---|---|---|
| MAT | 0.17$^{ns}$ | -0.14$^{ns}$ | -0.36$^{ns}$ | 0.02$^{ns}$ | 0.02 $^{ns}$ |
| MAP | **0.96***  | 0.11$^{ns}$ | 0.28$^{ns}$ | **0.93***  | **0.98**** |
| NPP | 0.2$^{ns}$ | 0.65$^{ns}$ | 0.39$^{ns}$ | 0.03$^{ns}$ | -0.10 $^{ns}$ |
| Sand | -0.66$^{ns}$ | 0.72$^{ns}$ | 0.55$^{ns}$ | -0.56$^{ns}$ | -0.70 $^{ns}$ |
| Silt | 0.38$^{ns}$ | **-0.91***  | -0.79$^{ns}$ | 0.29$^{ns}$ | -0.47 $^{ns}$ |
| Clay | **0.81**˙ | -0.51$^{ns}$ | -0.31 $^{ns}$ | 0.71$^{ns}$ | 0.80 $^{ns}$ |
| CEC | -0.67$^{ns}$ | -0.24$^{ns}$ | 0.03$^{ns}$ | 0.74$^{ns}$ | **0.82**˙ |
| pH | -0.74$^{ns}$ | -0.47$^{ns}$ | -0.31$^{ns}$ | -0.51 $^{ns}$ | -0.46$^{ns}$ |
| Fe | 0.24$^{ns}$ | 0.98* | 0.97**  | 0.98**  | -0.78$^{ns}$ |
| Al | 0.18$^{ns}$ | -0.16$^{ns}$ | -0.41$^{ns}$ | -0.17 $^{ns}$ | -0.17 $^{ns}$ |
| SWP | 0.70$^{ns}$ | 0.68$^{ns}$ | 0.70$^{ns}$ | - | - |
| Average Grain size | -0.25$^{ns}$ | **0.97***  | **0.88**˙ | 0.05 $^{ns}$ | -0.16 $^{ns}$ |

**Figures**
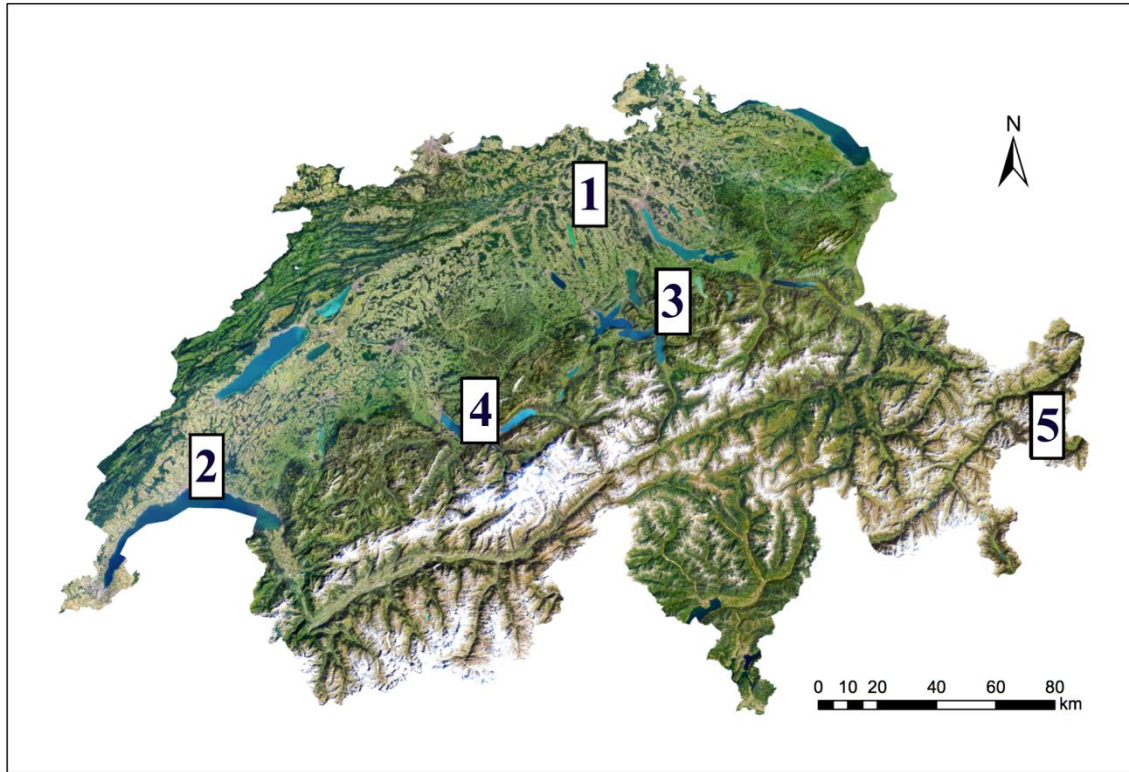
**Figure 1** Sample locations, all of which are part of the Long-term ecosystem research program (LWF) of the Swiss Federal Institute WSL, 1) Othmarsingen, 2) Lausanne, 3) Alptal, 4) Beatenberg and 5) Nationalpark Image made using 2016 swisstopo (JD100042).
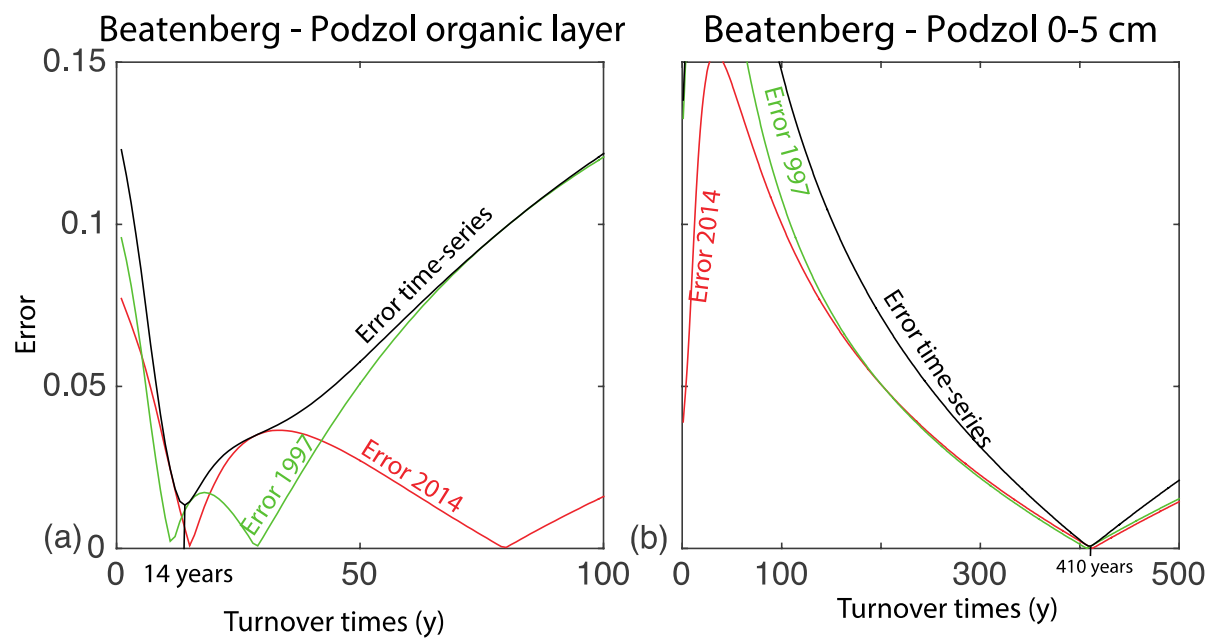
**Figure 2** Numerical optimization of least mean-square error reduction, showing and the reduction of error spread for two soil depths. For the Beatenberg Podzol organic layer (a) the individual ^{14}C time-points for both 1997 and 2014 both yield two solutions are almost equally likely (i.e. the error nears zero). The combined optimization using both the time-points reveal the likeliest option. For the (b) 0-5 cm layer the single time points only have a single likely solution.
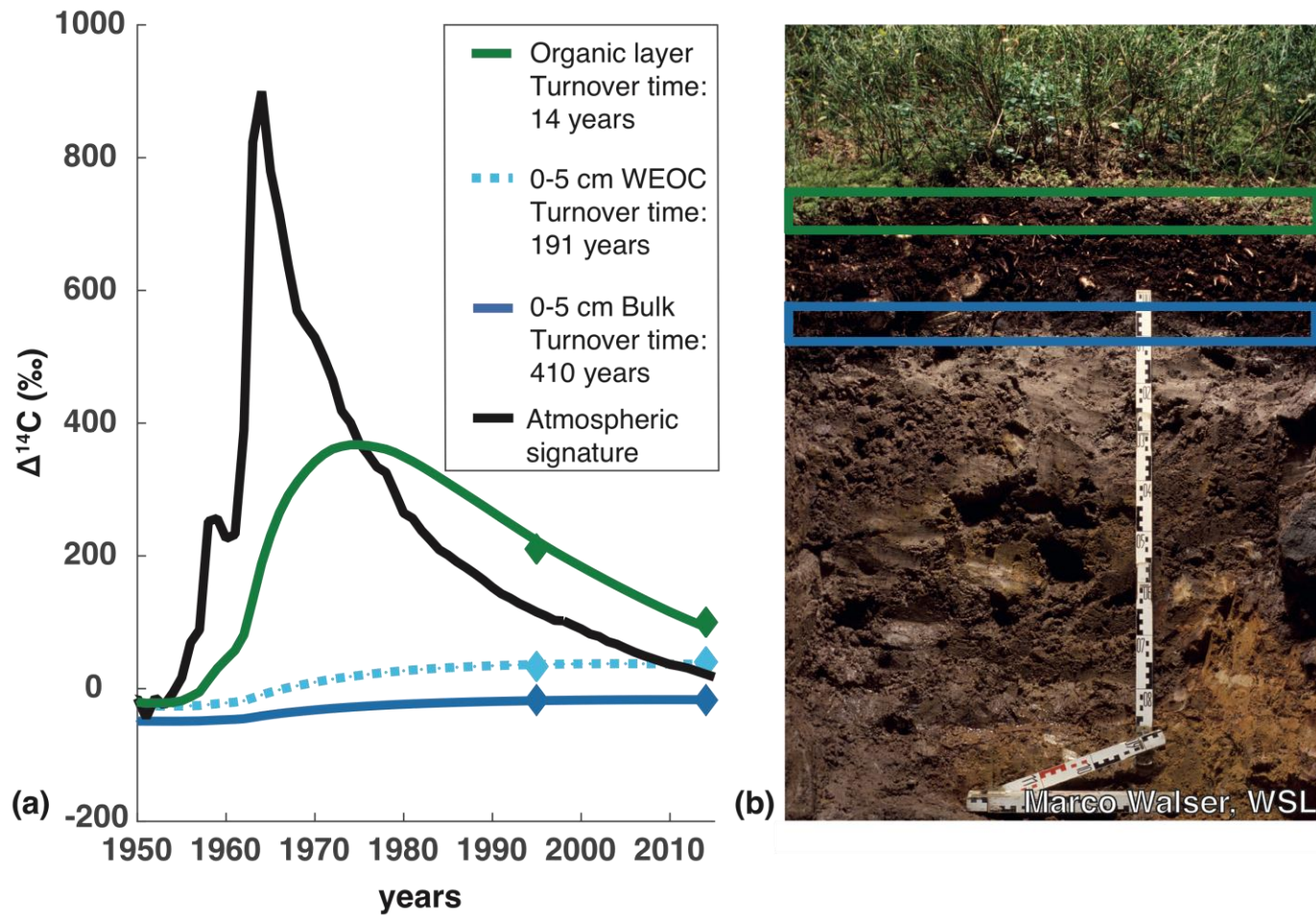
**Figure 3** (a) Time-series soil carbon turnover time in years (y) as determined by numerical modelling for (b) sub-alpine site Podzol Beatenberg. The bulk turnover time in the organic layer is rapid (14 years), followed by the turnover time of the water-extractable organic carbon (WEOC) (191 years) and the bulk turnover time of the soil (410 years) at 0-5 cm depth. Photo soil profile courtesy of Marco Walser, WSL.
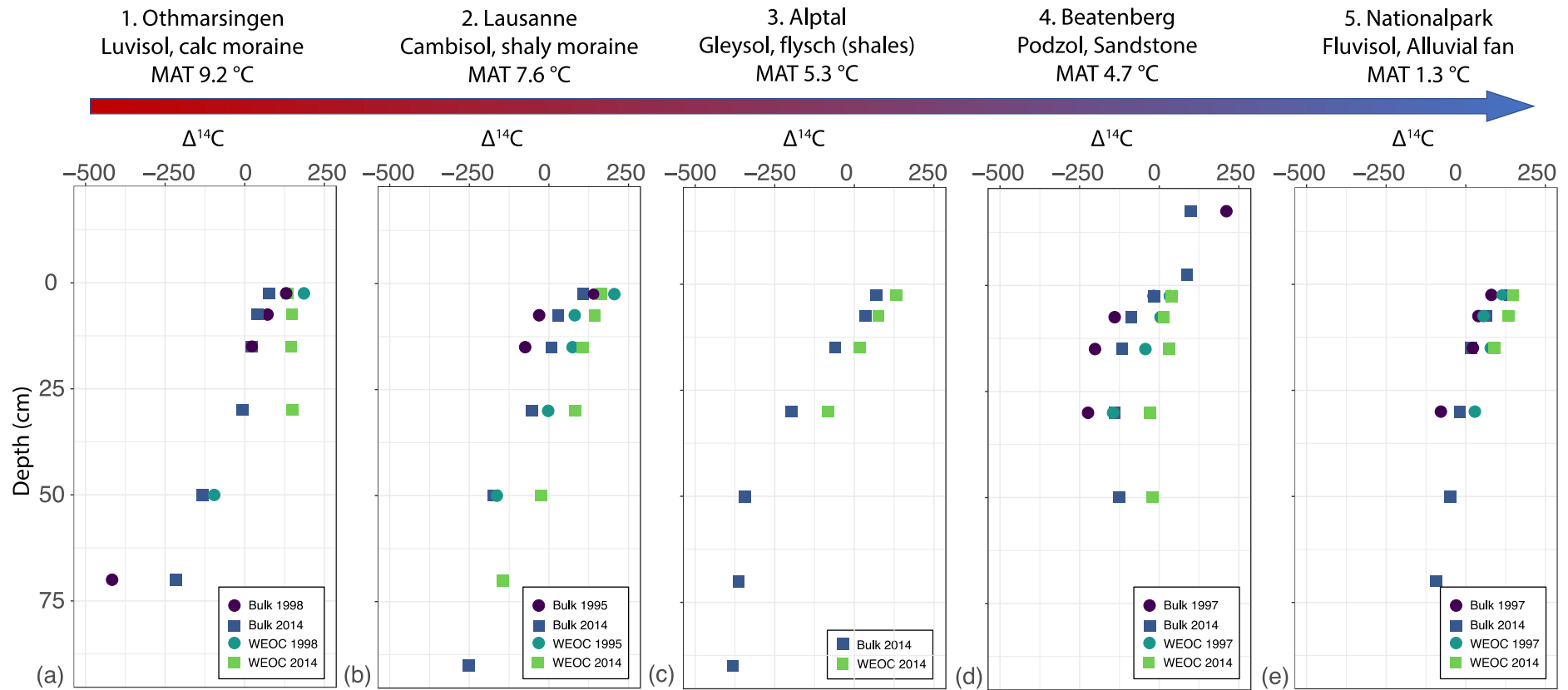
**Figure 4** (a-e) Changes in radiocarbon signature of both bulk soil and WEOC over two decades at four sites on a climatic gradient. For Alptal (Gleysol) (c) only the 2014 time-point was available. For the warmer locations Othmarsingen and Lausanne (Luvisol, Cambisol MAT 9.2-7.6 °C), depletion in bomb-derived radiocarbon occurs in the first five centimeters soil in 2014 as compared to 1995-8. The colder Beatenberg site (Podzol, MAT 4.7 °C) is marked by a clear enrichment of ^{14}C in the mineral soil in 2014 w.r.t. 1997. At the coldest site Nationalpark (Fluvisol, MAT 1.3 °C) almost all samples taken two decades after the initial sampling show an enrichment in radiocarbon signature. WEOC contains bomb-derived carbon in the topsoil in 2014 at all sites.
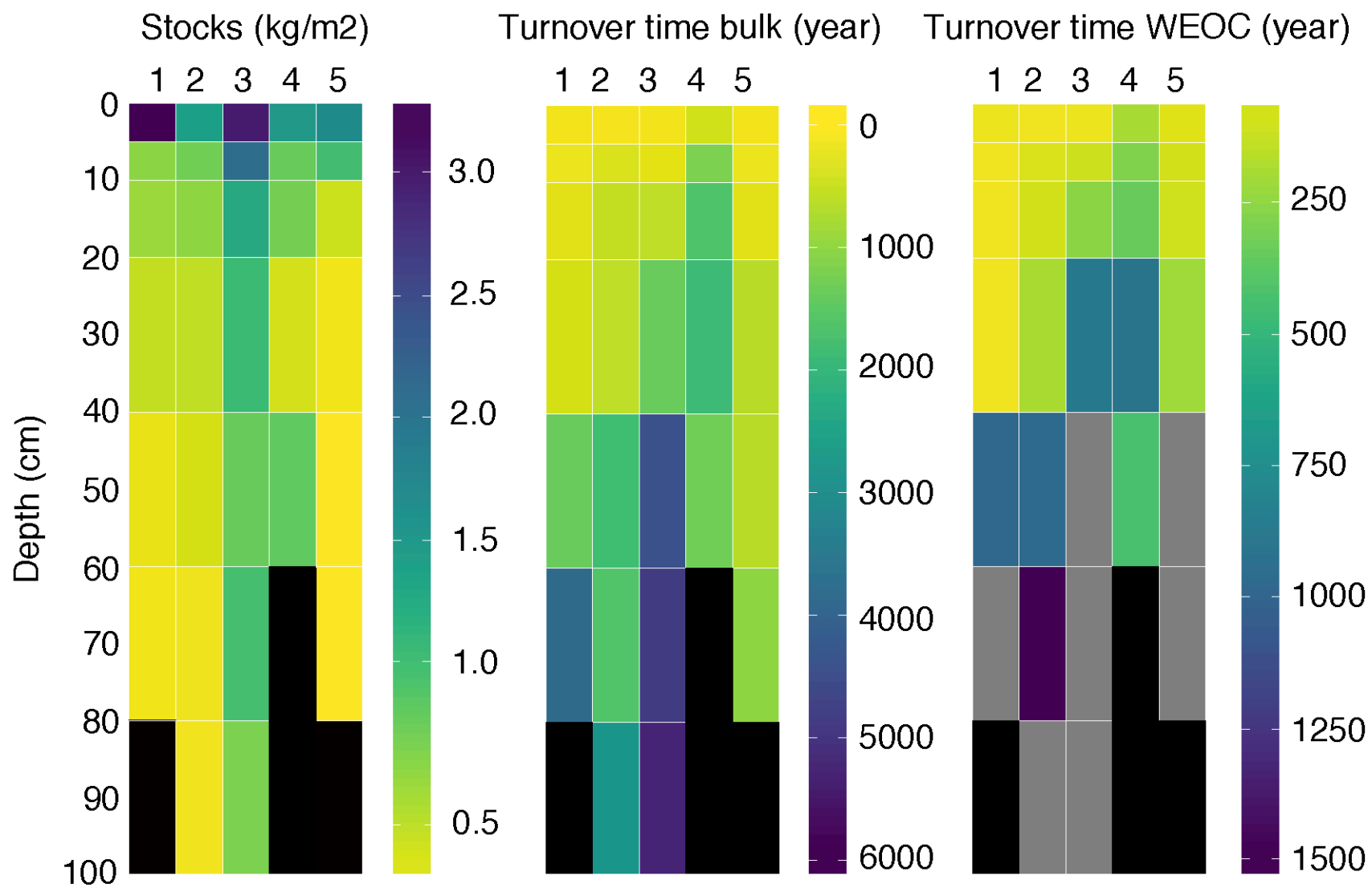
**Figure 5** Carbon (a) stocks in the mineral soil kgC/m$^2$, (b) turnover time bulk soil in years and (c) turnover time water extractable organic carbon soil in years. Locations are ordered from the warmest to coldest sites i.e. (1) Othmarsingen (Luvisol), (2) Lausanne (Cambisol), (3) Alptal (Gleysol), (4) Beatenberg (Podzol) and (5) Nationalpark (Fluvisol). Grey boxes indicate absence of material, black boxes indicate the occurence of the C-horizon (poorly consolidated bedrock-derived stony material or bedrock itself).
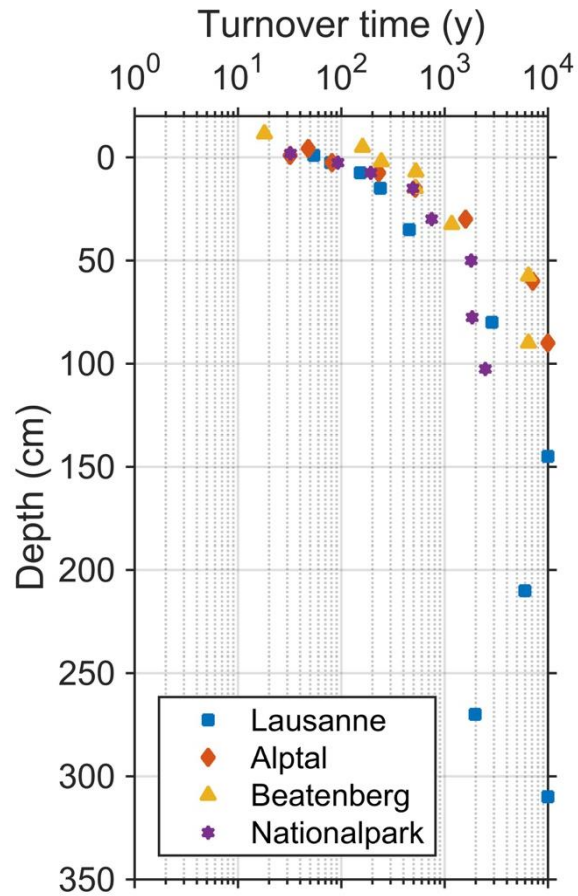
**Figure 6** Modeled turnover times (y) of single profiles sampled down to the bedrock between 1995 and 1998. $\Delta^{14}$C published in Van der Voort et al. (2016). Results indicate presence of petrogenic (bedrock-derived) carbon as modeled turnover time exceeds soil formation since the end of last ice age (10,000 years) in Lausanne (>100 cm, Cambisol) and Alptal (80-100 cm, Gleysol). For Beatenberg (Podzol) and Nationalpark (Fluvisol), no petrogenic carbon was found.